GYNECOLOGY

MicroRNA-30d deficiency during preconception affects endometrial receptivity by decreasing implantation rates and impairing fetal growth

Nuria Balaguer, PhD; Inmaculada Moreno, PhD; María Herrero; Marta Gonzáléz-Monfort; Felipe Vilella, PhD[1]; Carlos Simón, MD, PhD[1]

BACKGROUND: Maternal—embryonic crosstalk between the endometrium and the preimplantation embryo is required for normal pregnancy. Our previous results demonstrated that maternal microRNAs secreted into the endometrial fluid, specifically miR-30d, act as a transcriptomic regulator of the preimplantation embryo by the maternal intrauterine environment.

OBJECTIVE: To investigate the reproductive and fetal effects of murine miR-30d deficiency at the maternal—embryonic interface according to the origin of its maternal or embryonic default.

STUDY DESIGN: A miR-30d knockout murine model was used as the animal model to investigate the impact of maternal and/or embryonic origin of miR-30d deficiency on embryonic implantation and fetal development. Wild-type and miR-30d knockout pseudopregnant mice were used to study the effect of miR-30d deficiency on the receptivity markers by means of real-time quantitative polymerase chain reaction, immunofluorescence, and western blotting. We assessed receptivity markers and implantation rates in 6 different transfer conditions in which embryos obtained from wild-type, knockout, and knockout embryos pretreated with a miR-30d analog were transferred into either wild-type or knockout pseudopregnant females. The impact of miR-30d deficiency on fetal development was evaluated by analyzing the implantation sites and resorbing sites under physiological conditions at days 5, 6, 8, and 12 of pregnancy. Fetal growth was evaluated by analyzing fetuses and placentas at days 12 and 16 of pregnancy.

RESULTS: Maternal miR-30d deficiency induced a significant downregulation of endometrial receptivity markers. In wild-type recipients, miR-30d knockout embryos had poorer implantation rates than wild-type embryos (48.86 ± 14.33% vs 75.00 ± 10.47%, respectively, $P = .0061$). In miR-30d knockout recipients, the lowest implantation rate was observed when knockout embryos were transferred compared to wild-type embryos (26.04 ± 7.15% and 49.71 ± 8.59%, respectively, $P = .0059$). A positive correlation ($r = 0.9978$) was observed for maternal leukemia inhibitor factor expression with implantation rates. Further, the course of gestation was compromised in miR-30d knockout mothers, which had smaller implantation sites, greater rates of resorption, and fetuses with smaller crown-rump length and fetal/placental weight ratio.

CONCLUSION: Our results demonstrate that maternal and/or embryonic miR-30d deficiency impairs embryonic implantation and fetal development in the animal model. This finding adds a novel miRNA dimension to the understanding of pregnancy and fetal growth restriction in humans.

Key words: epigenetic, fetal growth restriction, implantation, maternal—embryonic crosstalk, microRNA, miR-30d, pregnancy, small for gestational age

Defects in the intrauterine environment can negatively impact the health of the fetus well into adulthood.[1] A key intrauterine factor is the bidirectional communication between the endometrium and the preimplantation embryo and, later, the fetus, to support both implantation and fetal development. Establishing adequate maternal—embryonic crosstalk is complex[2] and requires the coordination of both soluble embryo-derived factors and maternal secreted molecules.[3] Factors involved in this dialogue include chemokines, cytokines, adhesion molecules, and growth factors.[4–9]

MicroRNAs (miRNAs), which have emerged as novel regulators of cell—cell communication, are essential for regulating gene expression in fetal and maternal tissues during conception and through the course of pregnancy.[10,11] miRNAs contained within exosomes/microvesicles have been detected in human endometrial fluid, suggesting their potential role in embryo—maternal interactions during the early stages of implantation.[12,13] Moreover, a broad range of miRNAs has been linked with pregnancy-related disorders, such as implantation failure, preeclampsia, preterm labor, and intrauterine growth retardation.[14–20]

Several miRNAs are implicated in endometrial receptivity—hsa-miR-30b and -30d, which have been found to be upregulated, and hsa-miR-494, which is downregulated, during the window of implantation (WOI) in humans.[21] The predicted target genes of these miRNAs have been related to cyclic remodeling of the endometrium, including endometrial maturation to the receptive stage.[21] Our previous results demonstrated that endometrial miR-30d dysregulation during the WOI leads to abnormal implantation rates by impairing the expression of adhesion molecules (integrin subunit beta 3, integrin subunit alpha 7, and cadherin 5) in the trophectoderm cells of murine blastocysts.[12]

As a result of the pleiotropic effects caused by miRNAs, it is difficult to

Cite this article as: Balaguer N, Moreno I, Herrero M, et al. MicroRNA-30d deficiency during preconception affects endometrial receptivity by decreasing implantation rates and impairing fetal growth. Am J Obstet Gynecol 2019;221:46.e1-16.

0002-9378/$36.00

https://doi.org/10.1016/j.ajog.2019.02.047

AJOG at a Glance

Why was the study conducted?

Our laboratory previously demonstrated that maternal microRNAs, specifically miR-30d, secreted by the endometrium into the endometrial fluid act as transcriptomic regulator of the preimplantation embryo. Here, we aim to investigate in vivo at what extent the maternal and/or embryonic deficiency of this microRNA affects embryonic implantation and fetal development.

Key findings

Maternal and/or embryonic microRNAs miR-30d deficiency, especially when both are combined, impairs embryonic implantation and the fetal development. We identified a significant downregulation of leukemia inhibitory factor.

What does this add to what is known?

We demonstrate for the first time, in an animal model, the adverse effect of endometrial and/or embryonic miR-30d deficiency on reproductive and gestational outcomes, causing fetal growth restriction.

define the specific role of a particular miRNA. To date, most miRNA experiments have been conducted on a cellular level in vitro. Others have generated in vivo models by injecting miRNA mimics and/or inhibitors, producing phenotypic changes by means of transcriptional modifications on their specific predicted target genes. However, there are no in vivo models demonstrating the impact of a specific miRNA deficiency in the initiation of conception as well as during pregnancy, in a bidirectional communication context. Here, we use a miR-30d knockout (KO) mouse model to test the reproductive and fetal impact of the miR-30d deficiency at the maternal−embryonic interface and its relevance depending on whether the miR-30d deficiency originates from the maternal endometrium and/ or the embryo.

Materials and Methods

Experimental design

A miR-30d KO mouse model was used to investigate the impact of maternal and/or embryonic origin of miR-30d deficiency on implantation and fetal development. Wild-type (WT) and miR-30d KO pseudopregnant mice were used to study the effect of miR-30d deficiency on the receptivity markers using real-time quantitative polymerase chain reaction (RT-qPCR), immunofluorescence, and western blotting. We assessed receptivity markers and implantation rates in 6 different transfer conditions in which embryos obtained from WT, KO, and KO embryos pretreated with a miR-30d analog where transferred into either WT or KO pseudopregnant females. The impact of miR-30d deficiency on fetal development was evaluated by analyzing the implantation sites and resorbing sites under physiological conditions at days 5, 6, 8, and 12 of pregnancy. Fetal growth was evaluated by analyzing fetuses and placentas at days 12 and 16 of pregnancy.

Animal model

miR-30d KO mice were produced by the Jackson Laboratory (Bar Harbor, ME) from the miRNA cluster 26 (miR-30b/miR-30d) (MirC26tm1Mtm/Mmjax) on a mixed C57BL/6, Fvb, and 192P2 background. Mature mice were caged in a controlled environment with a cycle of 14L:10D. All animal procedures were approved by the Spanish Government Ministry of Agriculture, Livestock, and Fisheries of the Spain Government (Code: 2017/VSC/PEA/00005). To confirm the reproducibility of the results, at least 3 mice per group were used for each stage or treatment in this study.

Uterine sample collections to analyze endometrial receptivity

Uterine tissues were isolated from nonpregnant (day 0 [E0]), pseudopregnant (day 4 [E4], and day 5 [E5]) and pregnant (d4; and d5) WT and miR-30d KO that were synchronized in estrus following the protocol described by Moreno-Moya et al.[22] Three days later, some females were euthanized by cervical dislocation to harvest E0 samples, whereas the others were housed overnight with nonvasectomized mice or vasectomized mice at a ratio of 2 females per male. Females presenting vaginal plugs (classified as day 1 of pregnancy or pseudopregnancy) were separated and euthanized at day 4 or 5, as appropriate, to obtain uteri to analyze the receptivity markers by RT-qPCR (total uteri per time point: WT, n = 18; KO, n = 18), immunofluorescence of receptivity markers (total uteri per timepoint: WT, n = 9; KO, n = 9), and western blot to identify the generation of proteins related to the receptivity status (total uteri per time point: WT; n = 18; KO, n = 18).

Study of key endometrial receptivity markers by RT-qPCR

RT-qPCR was used to assess mRNA expression levels of key receptivity markers in nonpregnant and pseudopregnant females at days 4 and 5 of pseudopregnancy (WT, n = 18; KO, n = 18). RNA was extracted using the RNeasy Kit (QIAGEN, Hilden, Germany) and quantified using NanoDrop spectrophotometer (Thermo Fisher Scientific Inc, Waltham, MA). RT was performed using the PrimeScript RT reagent Kit (Perfect Real Time; Clontech Laboratories, Mountain View, CA), and qPCR was conducted using the "Kapa Sybr fast master mix universal 2x qPCR master mix" (Sigma Aldrich, St Louis, MO) in a QuantumStudio 5 Real-Time PCR system. Conditions for the qPCR were as follows: enzyme activation at 95°C for 10 minutes and 40 two-step cycles 10 seconds at 95°C and 30 seconds at 60°C. Fold changes were estimated using the $-2^{\Delta\Delta Ct}$ formula. Actin was used as a housekeeping control to determine the relative quantification of the analyzed genes. Primer sequences are presented in Supplemental Table 1.

Immunofluorescence assays of receptivity markers

Uterine tissues were isolated from nonpregnant (day 0 [E0]), pseudopregnant

(day 4 [E4], and day 5 [E5]) and pregnant (day 4 [E4] and day 5 [E5]) WT and miR-30d KO females (total uteri per timepoint: WT, n = 9; KO, n = 9), flash frozen, and stored in cryovials at −80°C. Next, tissues were completely embedded in an OCT compound before cryostat sectioning. Cryosections were cut at 7 mm onto poly-L-lysine−coated slides, rehydrated with phosphate-buffered saline (PBS), and fixed with 4% paraformaldehyde for 10 minutes. Permeation was performed with PBS-1% Triton X-100 for 10 minutes. Sections were blocked with 5% bovine serum albumin/0.05% triton/4% fetal bovine serum in PBS. Sections were then incubated with the following primary antibodies: cyclooxygenase-2 (COX2 [1 μg/mL], ref: ab15191; Abcam, Cambridge, United Kingdom), leukemia inhibitory factor (LIF [20 μg/mL], ref: ab11362; Abcam), Msh homeobox 1 (MSX-1 [1:200], ref: ab174207; Abcam), Msh homeobox 2 (MSX-2 [1:200], ref: HPA005652; Sigma-Aldrich, St. Louis, MO), estrogen receptor (ESR [1:200], ref: ab32063; Abcam), and progesterone receptor (PGR [1:200], ref: 8757; Cell Signaling Technology, Danvers, MA) O/N at 4°C in a humidified chamber. In addition to these primary antibodies, one against Zonula occludens 1 (Abcam) was used. Zonula occludens 1 is a tight junction protein often expressed in the primary decidual zone after implantation. It was used in this study to detect the region surrounding the implantation sites.

Sections were washed 3 times with PBS-0.05%TritonX-100/0.1% bovine serum albumin and incubated with a goat anti-rabbit IgG (H+L) Superclonal secondary antibody, Alexa Fluor 555 (Thermo Fisher Scientific). Nuclei were stained with 4,6-diamidino-2-phenylindole (Thermo Fisher Scientific). Aquatex (Merck-Millipore, Billerica, MA) was used as the mounting medium. Tissues from control (WT) and experimental uteri (KO) were processed on the same slide. Images were acquired with a 60 water immersion confocal microscope (FV1000; Olympus). Image processing was conducted by using Imaris software (Bitplane, Zurich, Switzerland). Measurements of the fluorescence intensity values (integrated density/area) were conducted with ImageJ software (National Institutes of Health, Bethesda, MD).

Protein extraction and western blot analysis for the markers of endometrial receptivity

Uteri were flash frozen, cut into pieces, and homogenized in 1 mL of lysis buffer following the protocol described by Moreno-Moya et al.[23] Samples were homogenized at 30-second intervals until completely dissociated (n = 6 uteri per condition tested and genotype analyzed; total uteri per time point: WT, n = 18; KO, n = 18). The tissue slurry was transferred into clean 1.5-mL Eppendorf tubes and allowed to incubate at 4°C for 1 hour. Samples were then centrifuged at 15,000 rpm (gravity 21,000 g) for 30 minutes. The supernatant was recovered, and protein concentrations quantified by a Bradford assay following the manufacturer's instructions. Then, 25 μg of each protein sample was heated in Laemli SDS sample buffer (6x; Alfa Aesar, Haverhill, MA) and separated by sodium dodecyl sulfate polyacrylamide gel electrophoresis followed by electroblotting onto polyvinylidene difluoride membranes (Bio-Rad Laboratories, Hercules, CA). Membranes were incubated overnight with specific primary (1:1000) antibodies diluted in 3% nonfat milk, following the manufacturer's specifications. Antibodies against mouse COX2 (1:1000, ref: ab1519; Abcam), LIF (1:500, ref: ab11362; Abcam), MSX-1 (1:200, ref: ab174207; Abcam), MSX-2 (1:500, ref: HPA005652; Sigma-Aldrich), ESR (1:1000, ref: ab32063; Abcam), PGR (1:500, ref: 8757; Cell Signaling Technology, Danvers, MA), and calnexin (1:1000, ref: ADI-SPA-860-F; Enzo Life Sciences, Farmingdale, NY) were used for western blotting. After 3 washes with 1% PBST, membranes were incubated with a 1:20,000 dilution of secondary antibodies (Santa Cruz Biotechnology, Dallas, TX). Finally, target proteins were detected by using the SuperSignal West Femto Chemiluminescent kit (Thermo Fisher Scientific).

Mouse embryo transfer assays

Female mice, ages 6−8 weeks, were primed to ovulate by administering 10 IU of pregnant mare serum gonadotropin (Sigma-Aldrich) and, 48 hours later, 10 IU of human chorionic gonadotropin (Sigma-Aldrich). Females were housed overnight with males and examined the following morning for the presence of a vaginal plug (classified as day 1 of pregnancy). On day 1.5 of pregnancy, the mice were euthanized by cervical dislocation and embryos flushed from the oviduct with PBS using a 30-gauge blunt needle. Embryos were then washed 3 times with fresh G2 Plus medium (Vitrolife, Göteborg, Sweden) and incubated in G2 medium for 72 hours at 37°C, 5% CO_2. For rescue experiments, 123 miR-30d KO embryos were pretreated with 400 nM of an analog of miR-30d for 72 hours (miScript miRNA Mimic, cat. no. MSY0000245; QIAGEN). Beyond this timepoint, embryos at the blastocyst stage were washed 3 times with PBS and used to perform the embryo transfer into both WT and KO pseudopregnant females synchronized in estrus, as described previously. Females presenting a vaginal plug (day 1 of pregnancy) either the same day or 48 hours after mating were separated to undergo embryo transfers on day 4. Six different transfer conditions were used to analyze the influence of both maternal and embryonic factors influencing the implantation process: (1) WT embryos transferred into WT recipients (WTE-WTR), (2) KO embryos into WT recipients (KOE-WTR), (3) miR-30-day pretreated KO embryos into WT recipients (PTKOE-WTR), (4) WT embryos into KO recipients (WTE-KOR), (5) KO embryos into KO recipients (KOE-KOR), and (6) miR-30d pretreated KO embryos into KO recipients (PTKOE-KOR).

These transfers were done using a Non-Surgical Embryo Transfer (NSET)

FIGURE 1
Receptivity markers in WT and miR-30d KO uteri at pre- and postimplantation

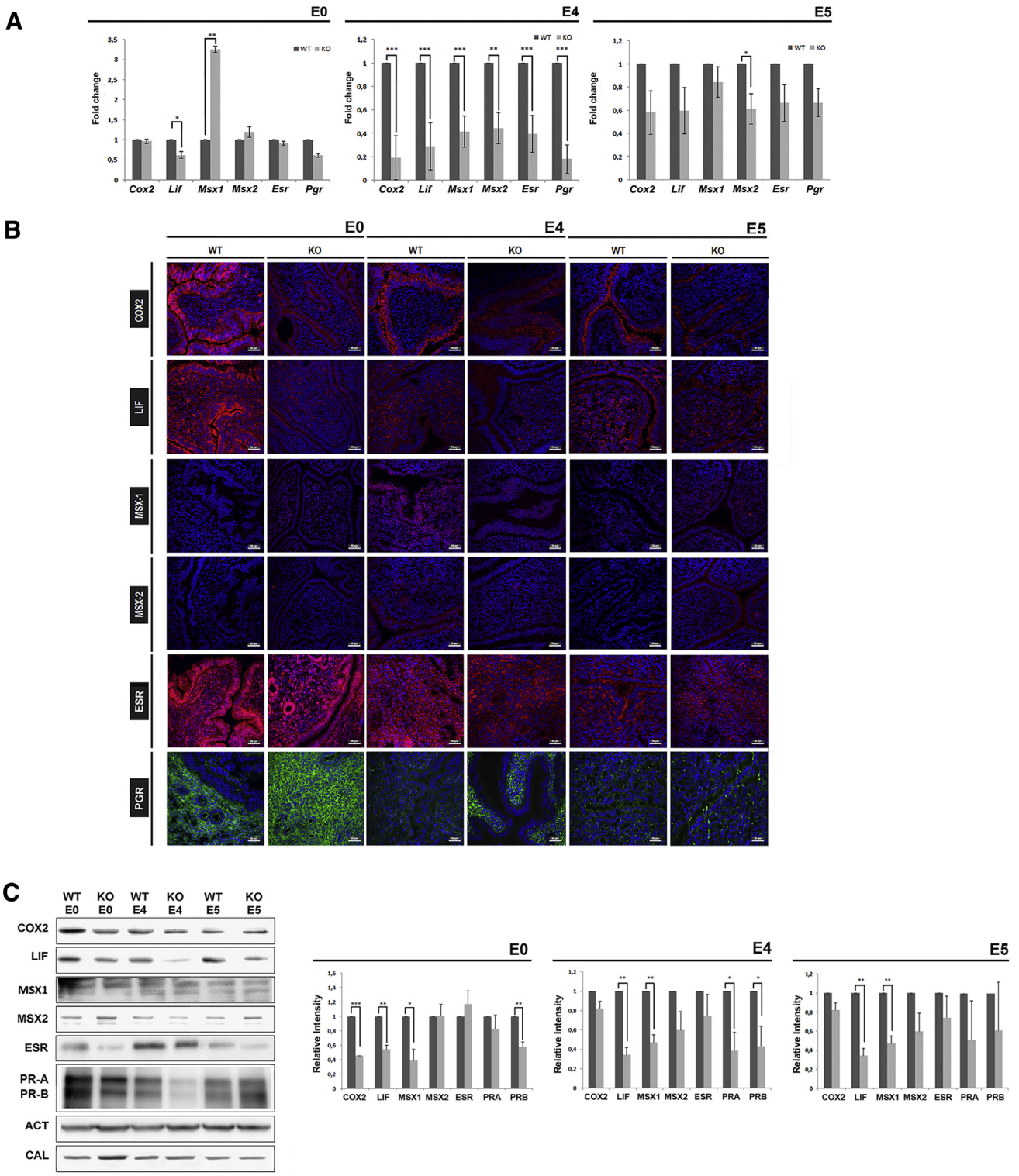

device for mice (ParaTechs, Lexington, KY). For each condition tested; an average of 10−15 embryos was transferred. Three biological replicates were performed for harvest on day 5 (embryos transferred per condition: ~36; total embryos transferred in the 6 conditions tested: ~216). Six biological replicates were performed for harvest on

day 6.5−7 of pregnancy (embryos transferred per condition: WTE-WTR [54]; KOE-WTR [87]; PTKOE-WTR [67]; WTE-KOR [73]; KOE-KOR [58]; PTKOE-KOR [84]; total embryos transferred in the 6 conditions tested: ∼423). Implantation sites were visualized using the colorant Chicago Sky blue (Sigma-Aldrich) injected via tail vein. Finally, females were euthanized by cervical dislocation and the implantation sites counted to calculate implantation rates. Uteri obtained from pseudopregnant females euthanized at day 5 of pregnancy were flash-frozen and stored in cryovials at −80°C. Cryosections and immunofluorescence analyses were performed following the protocol described previously (n = 3 uteri per condition tested and genotype analyzed; total uteri: WT, n = 6; KO, n = 6).

Characterization of the implantation phenotype and pregnancy outcomes associated with miR-30d deficiency

The course of gestation was evaluated in pregnant females on days 5, 6, 8, and 12. Specifically, on days 5 and 6, implantation sites were visualized by intravenous injection of a Chicago Sky blue (Sigma-Aldrich) solution, and the number of implantation sites—demarcated by distinct blue bands—was recorded (number of uteri evaluated: WT, n = 4; KO, n = 5). Resorption sites were identified at day 12 (number of uteri evaluated: WT, n = 10; KO, n = 5). In all cases, the size of the implantation sites was evaluated. The latter was determined considering the characteristic area of an ellipsoid (Eq. 1):

$$A = \pi \cdot \frac{D_1}{2} \cdot \frac{D_2}{2} \qquad (1)$$

Where A is the area (cm^2), D_1, the minor radius (cm), and D_2 the major radius (cm). Measures were done by image analysis with Adobe Photoshop (San Jose, CA) software (WT: E5 [n = 16]; E6 [n = 37]; E8 [n = 28]; E12 [n = 16]; KO E5 [n = 23]; E6 [n = 15]; E8 [n = 20]; E12 [n = 17]). Fetal growth restriction was evaluated by analyzing the fetuses and the placentas at day 12 and 16 of pregnancy (WT: E12 [n = 14]; E16 [n = 17]; KO: E12 [n = 12]; E16 [n = 5]). In fetuses, 2 parameters were assessed, crown-rump length (cm) and weight (mg). Placental weight also was evaluated and used to estimate the fetal weight:placental weight (FW:PW) ratio. Finally, parturition events were monitored from days 17 through 21 by observing mice 3 times daily: morning, noon, and evening. Pups were allowed to grow until weaning (21 days post-birth) and were then euthanized by cervical dislocation to record their weights (mg), widths (cm), and lengths (cm) (WT, n = 40; KO, n = 37).

Statistical analysis

Statgraphics Centurion software package (v.16.1.11; StatPoint Technologies, Inc, The Plains, VA) was used to compare results by one-way analysis of variance. Statistical significance was accepted at a P value < .05. Statistical analysis for the implantation rates analysis in the different transfer conditions was performed with the 2-proportion test (based on chi-square test). A P value <.05 was considered significant.

Results

MiR-30d deficiency impairs endometrial receptivity

To examine the effects of miR-30 deficiency on endometrial receptivity, we analyzed the expression of cyclooxygenase-2 (*Cox2*), leukemia inhibitory factor (*Lif*), Msh homeobox 1 (*Msx1*), Msh homeobox 2 (*Msx2*), estrogen receptor (*Esr*), and progesterone receptor (*Pgr*) in the mouse endometrium at days 0, 4, and 5 of pseudopregnancy. Thus, in the nonpregnant endometrium condition (E0), *Lif* mRNA levels were significantly reduced (P = .0355) and *Msx1* mRNA levels were increased in KO compared with WT tissues (P = .0014; Figure 1, A). Of note, all the receptivity markers were significantly reduced at the beginning of implantation (E4) in KO uteri, but once implantation was established (E5) differences remained significant only for *Msx2* (Figure 1, A).

To determine whether the mRNA expression changes also were reproduced at the protein level, immunofluorescence and western blot analyses were performed. The changes in the protein levels of COX2, LIF, and ESR were like those detected for their respective mRNAs over the time course (E0, E4, and E5; Figure 1, B) and the expression of these

A, RT-qPCRs performed on WT and miR-30d KO uteri samples during a nonpregnancy state (E0) and at day 4 (E4) and 5 (E5) of pseudopregnancy (n = 6 uteri per condition tested and per genotype analyzed; total uteri: WT, n = 18; KO, n = 18). Fold-change values are presented for all the analyzed receptivity markers (*Cox2*, *Lif*, *Msx1*, *Msx2*, *Esr*, and *Pgr*). Significant differences were observed at nonpregnancy state (*Lif* [P = .036]; *Msx1* [P = .001]), E4 (*Cox2* [P < .001]; *Lif* [P < .001]; *Msx1* [P < .001]; *Msx2* [P = .004]; *Esr* [P < .001]; *Pgr* [P < .001]), and E5 (*Msx2* [P = .0355]). **B,** Immunofluorescence assays performed on WT and miR-30d KO uteri in a nonpregnancy state, on day 4 and day 5 of pseudopregnancy (n = 3 uteri per condition tested and per genotype analyzed; total uteri: WT, n = 9; KO, n = 9). Micrographs suggest that COX2, LIF, and ESR expression was greater in the WT genotype than in the KO at all the stages analyzed. Staining was with Hoechst 33382 (*blue*): nucleus; Alexa Fluor 555 dye (*red*): receptivity markers COX2, LIF, MSX1, MSX2, and ESR; Alexa Fluor 488 dye (*green*): receptivity marker PGR. **C,** Western blot analysis performed on WT and miR-30d KO uteri at a nonpregnancy state, at day 4 and 5 of pseudopregnancy (n = 6 uteri per condition tested and genotype analyzed; total uteri: WT, n = 18; KO, n = 18). Significant differences were detected for COX2 (P < .001) at nonpregnancy, LIF at nonpregnancy (P = .002), day 4 of pseudopregnancy (P = .001) and day 5 of pseudopregnancy (P < .001), ESR (P < .001) at day 5 of pseudopregnancy, PRB isoform (P = .0046) at nonpregnancy and both isoforms (PRA, P = .0224; PRB, P = .0341) at day 4 of pseudopregnancy.

COX2, cyclooxygenase 2; *ESR*, estrogen receptor; *KO*, knockout; *LIF*, leukemia inhibitory factor; *MSX1*, Msh homeobox 1; *MSX2*, Msh homeobox 2; *PGR*, progesterone receptor; *PRA*, progesterone receptor isoform A; *PRB*, progesterone receptor isoform B; *RT-qPCR*, quantitative reverse transcription polymerase chain reaction; *WT*, wild type.

Balaguer et al. MicroRNA-30d deficiency during preconception affects endometrial receptivity by decreasing implantation rates and impairing fetal growth. Am J Obstet Gynecol 2019.

FIGURE 2
Characterization of the implantation phenotype associated with miR-30d deficiency

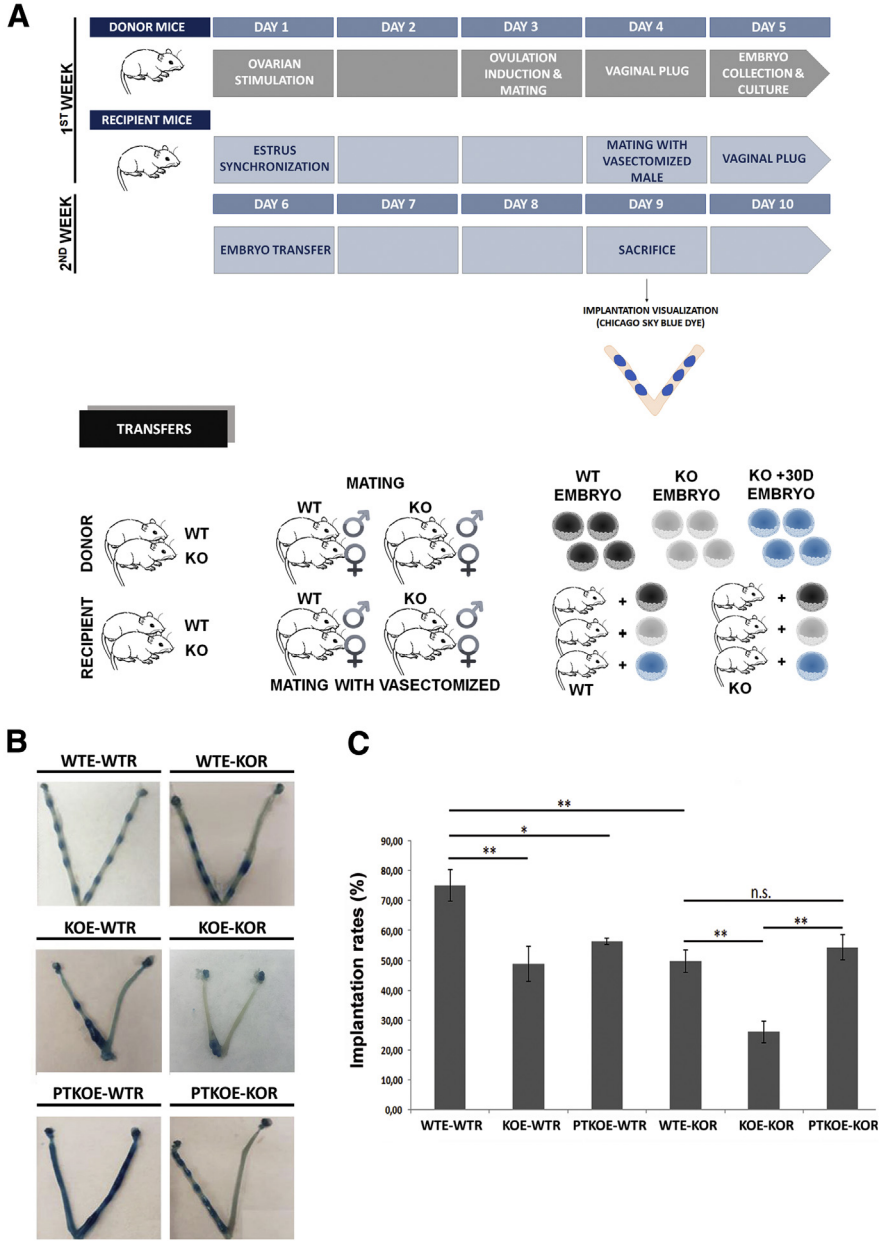

A, Schematic representation of the strategy preformed to conduct the different transfer combinations. **B,** Representative images of the implantation sites (demarcated by distinct *blue bands*) registered for the WT and KO uteri at days 6.5−7 of pregnancy. Six biological replicates were performed for day 6.5−7 of pregnancy (approximately 90 embryos transferred per condition; total of 423 embryos transferred in the 6 conditions tested). **C,** Implantation rate at day 6.5−7 of pregnancy. The implantation rates for KO embryos transferred into WT recipients was less than for the transfer of WT embryos into WT recipients (48.86% ± 14.33 vs 75.00% ± 10.47; $P = .008$); transfer of KO embryos into KO recipients led to lower implantation rates compared with the transfer of WT embryos into KO recipients (26.04% ± 7.15 vs 49.71% ± 8.59; $P = .007$); pretreating KO embryos with miR-30d significantly restored these implantation rates in KO uteri (54.39% ± 10.13 vs 26.04 ± 7.15; $P = .009$).

KO, knockout; *WT*, wild type.

Balaguer et al. MicroRNA-30d deficiency during preconception affects endometrial receptivity by decreasing implantation rates and impairing fetal growth. Am J Obstet Gynecol 2019.

markers was greater in WT than in KO uteri. WB analysis (Figure 1, C) revealed significant genotype-dependent differences between COX2, LIF, and MSX1 at E0, for LIF at E4, and for LIF and MSX1 at E5, whereas MSX2 was barely detectable in either genotype during implantation (Figure 1, B and C). Finally, with regard to PGR levels significant differences could be detected between both genotypes at day 0 for the PRB isoform ($P = .0046$) and for both isoforms (PRA, $P = .0224$; PRB, $P = .0341$) at day 4. (Figure 1, B and C).

MiR-30d deficiency reduces embryo implantation rates

Next, we investigated the reproductive phenotype according to the maternal or embryonic origin of the miR-30d deficiency. WT, miR-30d KO, and miR-30d KO embryos pretreated with 400 nM of synthetic miR-30d[12] were transferred into either WT or KO pseudopregnant mice in which estrus had been synchronized. The different conditions evaluated were as follows: (1) WT embryos transferred into WT recipients (WTE-WTR); (2) KO embryos into WT recipients (KOE-WTR); (3) miR-30d−pretreated KO embryos into WT recipients (PTKOE-WTR); (4) WT embryos into KO recipients (WTE-KOR); (5), KO embryos into KO recipients (KOE-KOR); and (6) miR-30d−pretreated KO embryos into KO recipients (PTKOE-KOR) (Figure 2, A).

Figure 2 reflects the implantation sites (Figure 2, B) and implantation rates (Figure 2, C) in uteri surgically removed at day 6.5−7 of pregnancy after these transfers were performed. Note that average and standard deviations are calculated from 6 biological replicates, with a total of 12−15 embryos per condition transferred in each replicate (total of 423 embryos transferred in 6 tested conditions).

KO embryos transferred into WT recipients had a lower implantation rates than WT embryos transferred into WT recipients (48.86 ± 14.33% vs 75.00 ± 10.47%, respectively; $P = .008$). Similarly, when transferred into KO recipients, KO embryos had lower implantation rates than WT embryos (26.04 ± 7.15% vs 49.71 ± 8.59%; $P = .0059$). Interestingly,

FIGURE 3
Receptivity markers in WT or KO uteri depending on the miR-30d source of origin

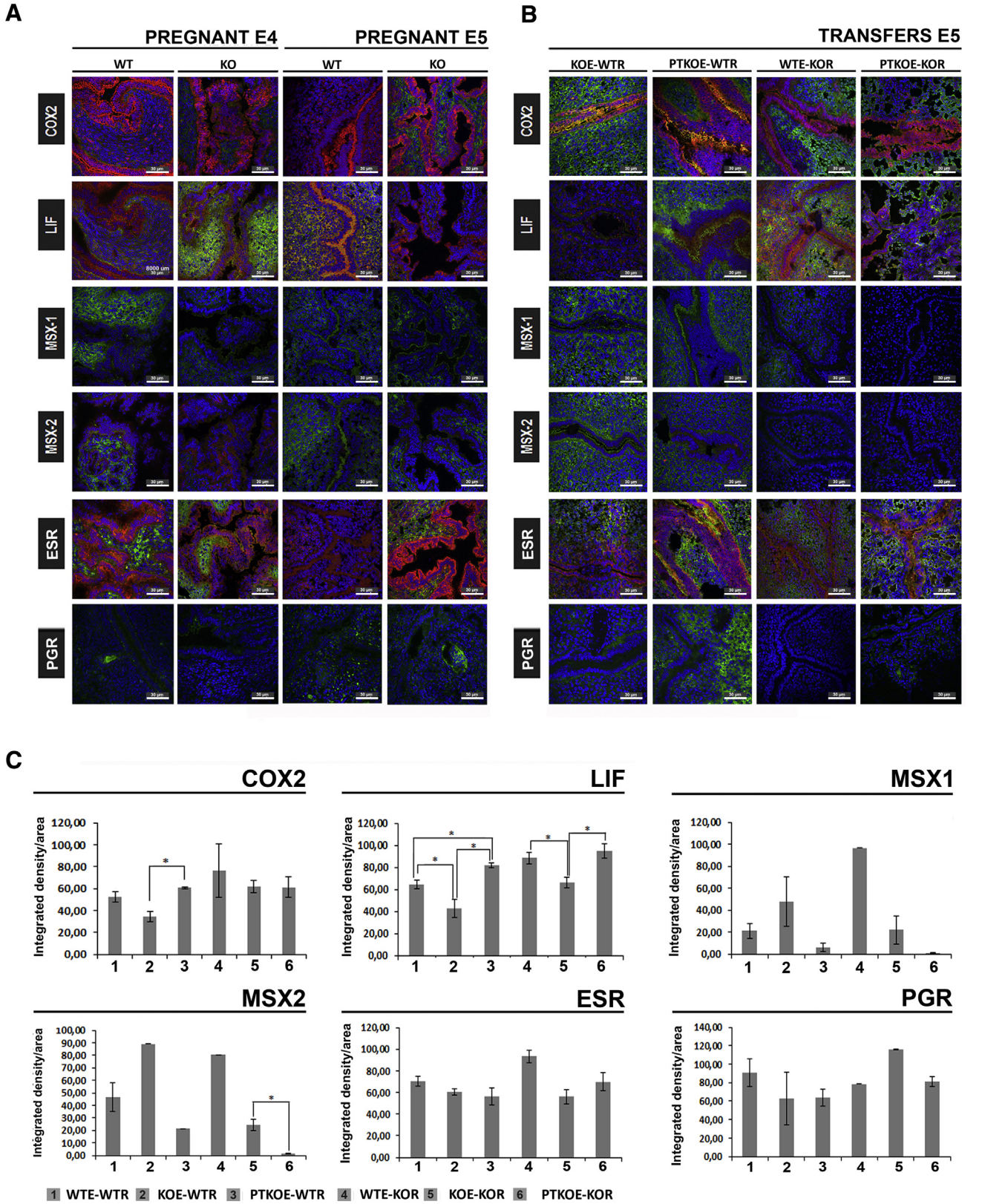

KO embryos pretreated with miR-30d and transferred into KO uteri had a greater implantation rate than untreated KO embryos (54.39 ± 10.13% vs 26.04 ± 7.15%, respectively; $P = .009$), but this rescue was not observed in WT uteri (56.26 ± 2.44% vs 48.86 ± 14.33%; $P = .749$; Figure 2, C), suggesting that the maternal and embryonic expression of miR-30d are equally important for achieving pregnancy.

To determine whether the implantation rates observed in the different conditions were associated with deregulation of receptivity markers during gestation, we evaluated marker expression on days 4 (E4) and 5 (E5) of pregnancy under physiological conditions (ie, with no embryo transfer) as compared to expression in the different transfer conditions indicated (Figure 1, A and B and Supplemental Figure 1). Under physiological conditions, the mean receptivity marker fluorescence intensity value on day 4 was lower in KO than WT samples; however, this generalized trend was not significant when the complete panel of micrographs from all the biological replicates was considered (Figure 3, A and Supplemental Figure 1). In contrast, on day 5 of pregnancy (E5) the fluorescence intensity value of LIF was significantly lower in the KO relative to the WT uteri (64.73 ± 3.86 and 49.15 ± 9.05, respectively; $P = .0336$; Supplemental Figure 1), although there were no statistically significant differences in expression for any other markers.

Yet, it is interesting to consider the implication of fluorescence intensity value patterns for endometrial–embryo communication in the different embryo transfer conditions (Figure 3, B and C). Although in some cases changes in the fluorescence intensity values failed to reach significance, the expression levels of LIF were significantly different in all the conditions tested (Figure 3, C). Thus, KO embryos transferred into either WT or KO mothers elicited considerably less LIF expression than WT embryos under the same conditions (WT uteri [42.82 ± 11.85 and 64.74 ± 8.63, respectively; $P = .0381$] and KO uteri [66.25 ± 9.05 and 88.54 ± 7.18, respectively; $P = .0061$]). Interestingly, treatment of KO embryos with a miR-30d analog before transfer normalized, or even increased, the mean fluorescence intensity value for LIF, regardless of whether the recipient uterus was WT or KO (WT uteri [miR-30d treated: 81.83 ± 3.49; untreated: 42.82 ± 11.85; $P = .0467$ and KO uteri [miR-30d treated: 94.50 ± 9.31; untreated: 66.25 ± 9.05; $P = .0046$]). Finally, COX2 exhibited perhaps the most intriguing changes. miR-30d pretreatment of KO embryos significantly increased the COX2 fluorescence intensity values in WT hosts (miR-30d treated: 34.52 ± 6.40; vs untreated 60.54 ± 1.24, $P = .0299$), thus recovering or exceeding the basal conditions (Figure 3, C).

Notably, the implantation rate pattern of the different transfer conditions coincided with the LIF mean fluorescence intensity value pattern (Figure 4, A), and there was a positive correlation ($r = 0.9978$) between the LIF mean fluorescence intensity value and the implantation rate for KO recipients (Figure 4, B).

MiR-30d deficiency induces fetal growth restriction

Considering the observed changes in maternal–embryo communication, we hypothesized that mir-30d deficiency in the mother or embryo would also affect placentation and fetal development. Implantation sites size and the number of resorptions were first assessed on days 5, 6, 8, and 12 of pregnancy in both WT and KO genotypes under physiological conditions. The implantation sites sizes were significantly smaller ($P < .001$) in KO mothers at all time points analyzed (Figure 5, A). Likewise, the number of resorptions identified by day 12 of pregnancy was slightly greater in KO females compared with the WTs (25% and 10%, respectively; Figure 5, B).

To determine whether these defects impact fetoplacental growth, we analyzed fetuses and placentas on day 12 (E12) and 16 (E16) of pregnancy (Figure 5, C and D). Placentas and fetuses obtained from KO females were significantly smaller ($P < .001$) in terms of crown-rump length ($P < .001$) and

A, Micrographs of WT and KO uteri at day 4 and 5 of pregnancy. Representative images for every receptivity marker are presented (n = 3 uteri per condition tested and per genotype analyzed; total uteri: WT; n = 6; KO, n = 6). Staining was with Hoechst 33382 (*blue*): nucleus; Alexa Fluor 555 dye (*red*): receptivity markers COX2, LIF, MSX1, MSX2, and ESR; Alexa Fluor 488 dye (*green*): from rows 1 to 5, represents the zonula ocludens-1 location. In row 6, Alexa Fluor 488 demarcates PGR expression. **B,** *Right panels*: Micrographs of WT and KO uteri in the different transfer conditions tested. For every condition tested; an average of 10–15 embryos were introduced. Three biological replicates were performed for day 5 of pregnancy; approximately 36 embryos transferred per condition tested. The staining was Hoechst 33382 (*blue*): nucleus; Alexa Fluor 555 dye (*red*): receptivity markers COX2, LIF, MSX1, MSX2, and ESR; Alexa Fluor 488 dye (*green*): rows 1–5 represents the zonula ocludens-1 location. In row 6, Alexa Fluor 488 demarcates PGR expression. **C,** Integrated fluorescence density/area calculated for every transfer condition tested: (1) WTE-WTR; (2) KOE-WTR; (3) PTKOE-WTR; (4) WTE-KOR; (5) KOE-KOR; and (6) PTKOE-KOR. Compared with WT embryos, transfer of KO embryos significantly reduces the presence of LIF in both WT and KO uteri (WT uteri [42.82 ± 11.85 vs 64.74 ± 8.63; $P = .038$ and KO uteri [66.25 ± 9.05 vs 88.54 ± 7.18; $P = .006$]). Transfer of miR-30d–pretreated KO embryos results in an increase of the LIF mean fluorescence intensity value in both WT and KO recipients (WT uteri [81.83 ± 3.49 vs 42.82 ± 11.85; $P = .047$ and KO uteri [94.50 ± 9.31 vs 66.25 ± 9.05; $P = .005$]). Transfer of miR-30d–pretreated KO embryos increases the COX2 mean fluorescence intensity values compared to transferring KO embryos to WT recipients (34.52 ± 6.40 vs 60.54 ± 1.24, $P = .03$).

COX2, cyclooxygenase 2; *ESR*, estrogen receptor; *KO*, knockout; *KOE-KOR*, KO embryos transferred into KO recipients; *KOE-WTR*, KO embryos transferred into WT recipients; *LIF*, leukemia inhibitory factor; *MSX1*, Msh homeobox 1; *MSX2*, Msh homeobox 2; *PGR*, progesterone receptor; *PTKOE-KOR*, miR-30-d–pretreated KO embryos transferred into KO recipients; *PTKOE-WTR*, miR-30-d–pretreated KO embryos transferred into WT recipients; *RT-qPCR*, quantitative reverse transcription polymerase chain reaction; *WT*, wild type; *WTE-KOR*, WT embryos transferred into KO recipients; *WTE-WTR*, WT embryos transferred into WT recipients.

Balaguer et al. MicroRNA-30d deficiency during preconception affects endometrial receptivity by decreasing implantation rates and impairing fetal growth. Am J Obstet Gynecol 2019.

FIGURE 4
Correlation between implantation rates and LIF staining under the different maternal transfer conditions

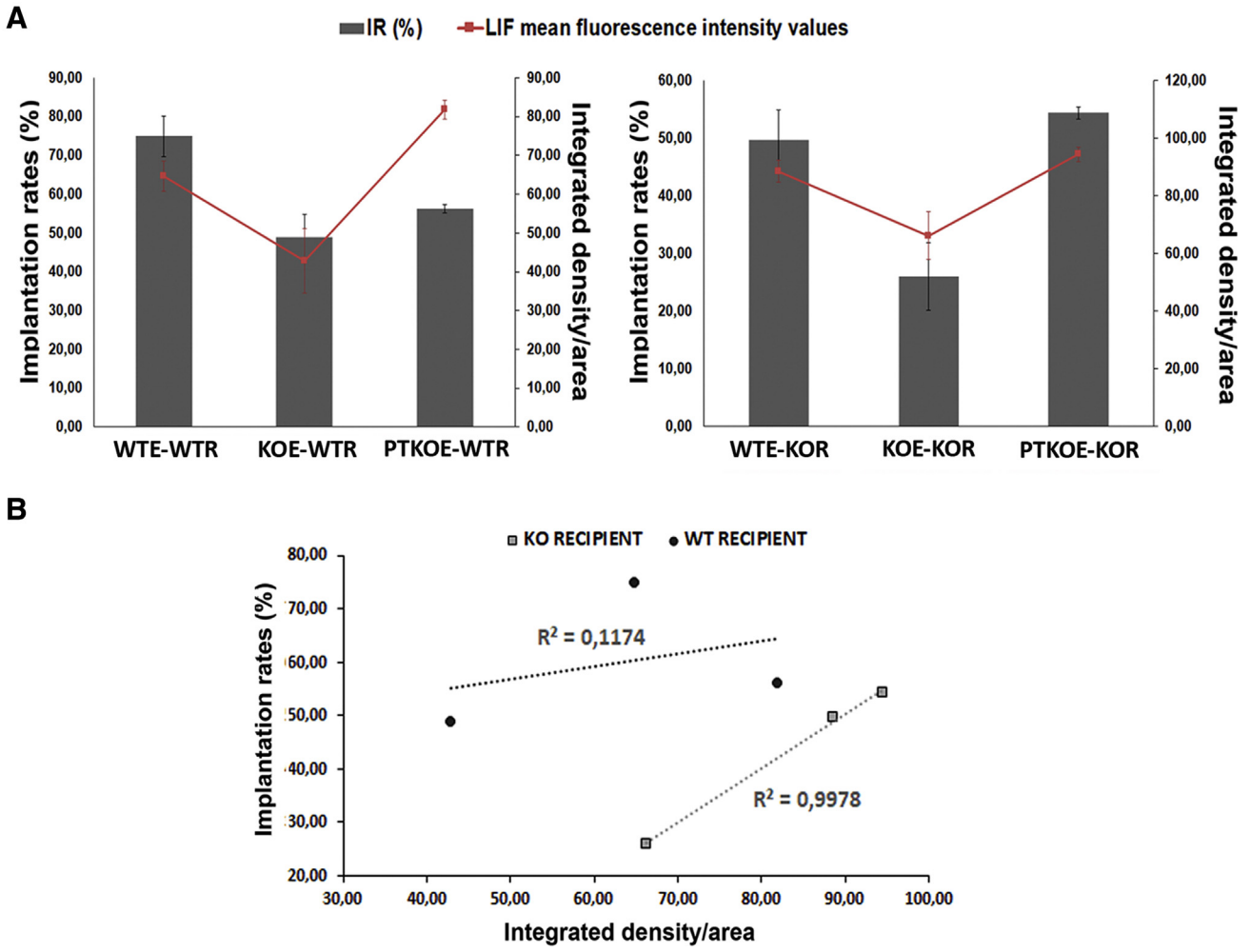

A, Graphs representing the overlapping tendency between the mean fluorescence intensity values for LIF (*red line*) and implantation rates (*gray bars*) observed for the WT (*left graph*) and KO (*right graph*) recipient. Primary axis: implantation rate (%), secondary axis: integrated density/area. **B,** Correlation between the LIF mean fluorescence intensity values and implantation rates (%) observed in all the transfer conditions tested. A positive correlation was found for the KO recipients (r = 0.998).

KO, knockout; *LIF*, leukemia inhibitory factor; *WT*, wild type.

Balaguer et al. MicroRNA-30d deficiency during preconception affects endometrial receptivity by decreasing implantation rates and impairing fetal growth. Am J Obstet Gynecol 2019.

FW:PW ratio (FW:PW at E12 [$P = .012$] and FW:PW at E16 [$P = .001$]), compared with WT females (Figure 5, C–F). The fetal/placental weight ratio is a proxy for placental efficiency,[24] defined as the grams of fetus produced per gram of placenta. These results suggest that miR-30 deficiency might affect the nutrient supply, resulting in smaller offspring. This hypothesis is supported by the observation that the weight (Figure 5, G and H), length (Figure 5, G and I), and width (Figure 5, G and J) of weaned offspring derived from KO dams were also significantly less than the controls ($P \leq .05$).

Comment

The importance of the intrauterine environment encountered during preconception and fetal development is key and any dysregulation might negatively affect adult life by increasing its risk of suffering noncommunicable diseases in adulthood.[1] This maternal–embryonic communication is reciprocal because embryo-derived factors profoundly affect maternal physiology during and after pregnancy.[3,13] Therefore, the nature of this preconception bidirectional relationship deserves further attention as key contributing to a successful pregnancy.[2]

In humans, the uterus is nonresponsive to blastocysts during the prereceptive phase of the menstrual cycle and becomes receptive during a short period of time in the mid-luteal phase known as the WOI in which the uterine

FIGURE 5
Pregnancy outcome associated with miR-30d deficiency

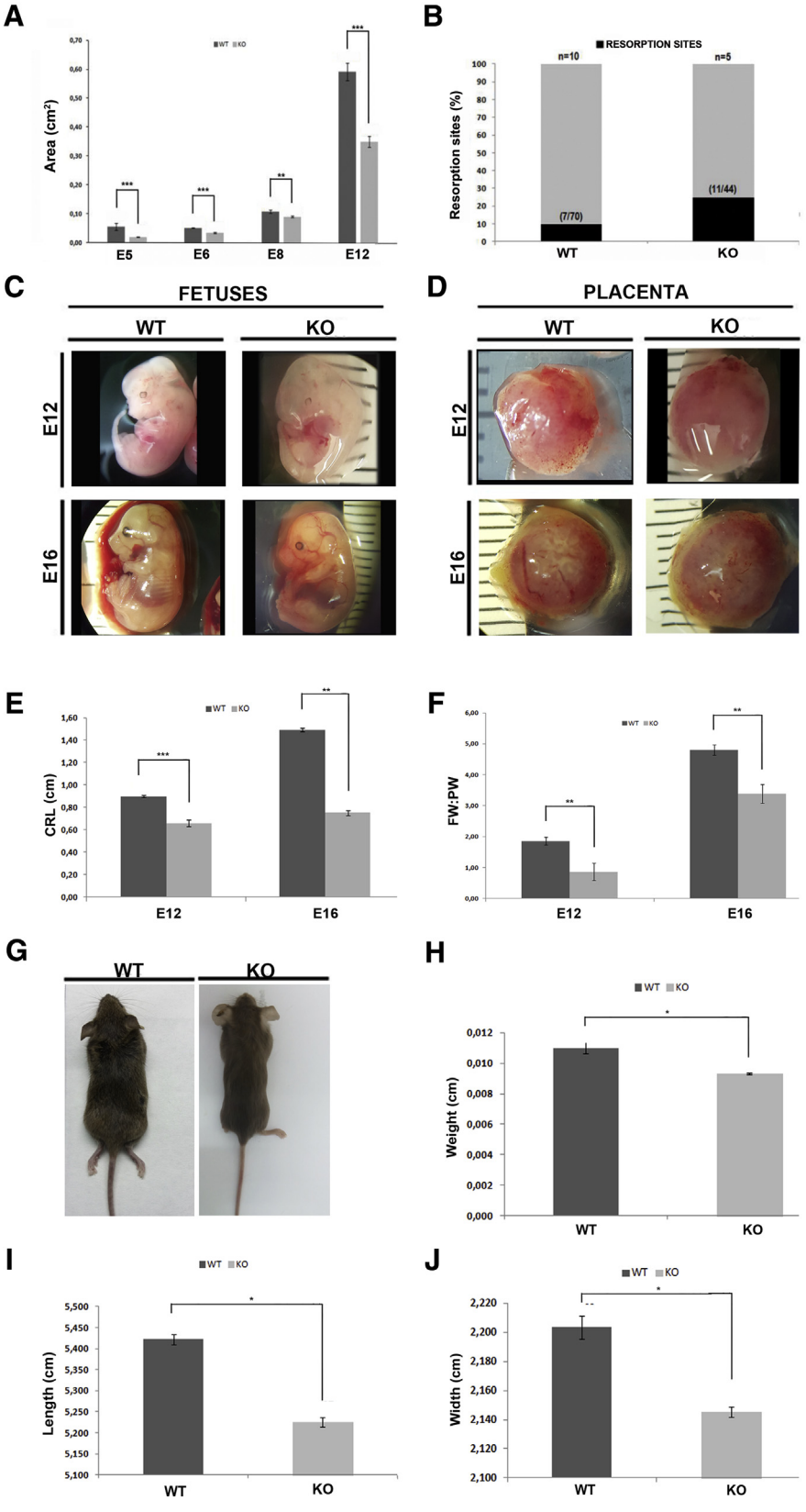

A, Implantation site size calculated throughout gestation (days 5, 6, 8, and 12) as measured by Adobe Photoshop image analysis software (WT: E5 [n = 16]; E6 [n = 37]; E8 [n = 28]; E12 [n = 16]; KO E5 [n = 23]; E6 [n = 15]; E8 [n = 20]; E12 [n = 17]). The implantation site sizes were significantly smaller (E5, E6, E8, E12; $P < .001$) in the KO genotype on all the gestation days analyzed. **B,** Resorption sites registered on day 12 of pregnancy (WT [n = 10], KO [n = 5]; n is the number of mice analyzed). In the graphs, between brackets, the number of resorption sites in relation to the total number of implantations sites analyzed is reflected. **C,** Fetal growth restriction was evaluated by analyzing the fetuses and the placentas on day 12 and 16 of pregnancy (WT: E12 [n = 14]; E16 [n = 17]; KO: E12 [n = 12]; E16 [n = 5]). Representative images of the fetuses obtained for the WT and KO genotypes on day 12 and 16 of pregnancy. **D,** Representative images of the placentas obtained for the WT and KO genotypes on day 12 and 16 of pregnancy. **E,** CRL determination for WT and KO genotype embryos on day 12 and 16 of pregnancy. There was a significant reduction in the RCL in the KO genotype on both days (CRL E12 [$P < .001$]; CRL E16 [$P < .001$]). **F,** The FW:PW ratio estimated for the WT and KO genotypes on day 12 and 16 of pregnancy. A significant reduction in the FW:PW ratio was observed in the KO genotype on both days (FW:PW ratio E12 [$P = .012$]). **G,** Representative images of weaned WT and KO mice (WT [n = 40]; KO [n = 37]). **H,** Weight determination for WT and KO weaned mice after 4 weeks of delivery; there were significant differences between these genotypes ($P = .05$). **I,** Length determination for weaned WT and KO mice 4 weeks after delivery; significant differences between these genotypes were detected ($P = .05$). **J,** Width determination for WT and KO weaned mice 4 weeks after delivery; significant differences between these genotypes were detected ($P = .05$).

CRL, Crown-rump length; *FW*, fetal weight; *KO*, knockout; *PW*, placental weight; *WT*, wild type.

Balaguer et al. MicroRNA-30d deficiency during preconception affects endometrial receptivity by decreasing implantation rates and impairing fetal growth. Am J Obstet Gynecol 2019.

epithelium is remodelled at the structural and functional levels to accept the adhesion of the embryo.[25] Likewise, murine uterus is not receptive during days 1−3 of the estrous and acquires receptivity on day 4 of pregnancy or pseudopregnancy.[26,27] Among other molecules, miRNAs are essential regulators of gene expression in fetal and

maternal tissues following conception and over the course of pregnancy. A broad range of miRNAs appear to be linked with endometrial receptivity, implantation, placental function, and parturition in both humans and mice.[14]

Principal findings of the study

The major finding of this study is that miR-30d originated either from the maternal endometrium and/or the embryo during preconception is implicated in the acquisition of endometrial receptivity, embryo implantation and fetal development.

The analysis of the expression of essential receptivity markers (*Cox2*, *Lif*, *Msx1*, *Msx2*, *Esr*, and *Pgr*) in the presence or absence of miR-30d demonstrate a significant difference in mRNA levels in the early stages of receptivity in KO compared with WT animals. Surprisingly, this difference was not observed in the late stages. Moreover, LIF protein levels were reduced in miR-30d KO uteri throughout the WOI. This deregulation during the preconception period was accompanied by decrease implantation rates at days 6.5−7 of pregnancy, suggesting that a miR-30d-transfer deficiency between the mother and the embryo impaired implantation.

The examination of the implantation phenotype in different maternal−fetal communication contexts, in which the mother and/or the embryo lacked miR-30d, revealed that blocking the transfer of miR-30d from the mother to the embryo or vice versa, significantly reduced the implantation rates achieved. Of note, impaired implantation was substantially recovered in the KO genotype after transferring KO embryos pretreated with a miR-30d analog.

Also, the absence of miR-30d in pregnant females affects fetal growth, as reflected in the generation of smaller implantation sites and greater rates of resorption in KO uteri, as well as a significant decrease in the embryonic crown-rump-length and fetal weight/placental weight ratio parameters. Thus, the offspring from KO-genotype mice are smaller than those from the WT genotype.

Results in context of what is known

Different studies on the role of miRNAs in human reproduction and obstetrics have reported that specific sets of miRNAs are differentially regulated in the endometrium at the time of embryo implantation.[12,21,28,29] Specifically, endometrial epithelial cells express greater levels of miR-30d during the receptive phase in both mice and humans.[12,28,29] These results are consistent with those of Sha et al, showing that miR-30b and miR-30d are upregulated in the luteinizing hormone + 7 (receptive [state]) versus luteinizing hormone + 2 (prereceptive [state]) endometriun of infertile women,[30] and downregulated in decidualized stromal cells versus non-decidualized cells.[31] Dysregulation of miR-30d has been associated to pregnancy complications in humans, as increased levels of miR-30d are found in patients with preeclampsia and fetal growth restriction compared with healthy pregnancies.[32,33] Our study analyzes the reproductive and fetal effect of bidirectional miR-30d deficiency in vivo in the preconception period and its subsequent effect on gestation and fetal development.

Clinical implications

Defective implantation leads to adverse "ripple" effects throughout pregnancy, including impaired fetoplacental growth.[34-36] Consistent with this, implantation sites in miR30d-KO females were significantly smaller at all time points analyzed. Based on the crown-rump length and FW:PW analysis, these fetuses exhibited retarded fetoplacental growth. These results suggest that miR-30d deficiency is associated with a modest effect on placental development.

Some pregnancy disorders initiate at the level of defective decidualization arising from epithelial-to-mesenchymal transition alterations.[37-39] LIF is an important regulator of this process; the uteri of *Lif*-null mice do not decidualize, even after using different well-established stimuli that induce this process.[40] The phenotype observed in the miR-30d KO could result from a succession of events triggered by LIF deficiency. However, miRNAs promiscuously regulate different mRNAs,[41] and miR-30d−deficient phenotypes also could be derived from the pleiotropic targets of this miRNA. Therefore, because current experiments only examine a limited range of this miRNA's potential range of action, further investigation and more data will be required to elucidate the full range of miR-30d regulation. However, what is clear is that depending on the source of miR-30d deficiency, the deleterious impact on the implantation process varies, highlighting the importance of optimal bidirectional communication in the preconception. Hence, this work opens the door for the investigation of the role of miR-30d in fetal growth restriction.

Research implications

It is generally assumed that miRNAs negatively regulate mRNA expression. However, this is not the first time that a member of the miR-30d family has been implicated in physiological contexts in which the absence of one of its members causes protein downregulation.[42] These observations suggest that miR-30d could be involved in managing protein balance, depending on internal or external stimuli. As a result, fundamental cellular processes including cell-cycle regulation, gene expression, apoptosis, and signal transduction could be compromised.[43,44] Hence, given the possible impairment of protein expression in the miR-30d KO model, variation in receptivity marker expression was evaluated in a maternal−fetal crosstalk context regulated by bidirectional miR-30d transfer. With that purpose, different embryo-transfer combinations were performed in both WT and KO females to cover all the possible maternal−embryo crosstalk scenarios. Interestingly, the variation in implantation rate among the mice in the different transfer conditions coincided with that observed for the mean fluorescence intensity values for LIF. Furthermore, there was a positive correlation between the mean fluorescence intensity value for LIF and the implantation rate registered, suggesting LIF as a potential indirect miR-30d target. LIF is an

essential regulator of embryo implantation in mice and is a crucial receptivity marker in several mammalian species, including humans.[45] Deregulation of LIF expression has been linked to several cases of female infertility associated with defective implantation.[46-48] Other researchers have suggested that LIF is regulated by miRNAs. The LIF mRNA expression pattern has been found to be virtually the inverse of miR-181a and miR-181b expression during pregnancy.[49] In addition, administering miR-181a or miR-181b mimics to mice led to decreased LIF mRNA and protein levels in their uteri on day 4 of pregnancy. Likewise, miR-223-39 has been described to affect embryo implantation by suppressing the expression of LIF and pinopodes in the endometrium of pregnant mice.[50]

Yet, it is important to consider that most researchers studying the role of miRNAs in endometrial receptivity highlight the effect exerted by the endometrium on the embryo but not how this might influence the acquisition of endometrial receptivity. To date, the closest described in the literature is that of human endometrial epithelial cells, which were able to acquire fluorescently-tagged miR-661, a miRNA present in nonimplanted blastocyst-conditioned medium.[51] Extracellular miR-661 reduce trophoblast spheroid adhesion to human endometrial epithelial cells, thus establishing a functional role for extracellular miRNAs in the maternal—fetal interface. Similarly, infusion of fluorescently labeled embryo-derived extracellular vesicles into the uterine horns of ewes near the time of implantation resulted in the detection of fluorescence in the cytoplasm of the uterine luminal and glandular epithelium.[52] These studies established that extracellular miRNAs originating from the embryo are internalized by uterine cells and modulate maternal gene expression, highlighting the presence of a functional signaling role between the blastocyst and maternal endometrium during the WOI. In this context, here we show evidence that miRNAs transferred from early developmental-stage embryos impact endometrial function, influencing levels of LIF as well as embryo implantation rates.

The observed miR-30d—associated phenotypes, particularly those evident during implantation, might arise from altered epithelial-to-mesenchymal transition. Recent studies have suggested that epithelial-to-mesenchymal transition during implantation is partially regulated by the abundance of miR-30d.[53] Specifically, reduced miR-30d expression promotes epithelial-to-mesenchymal transition and invasiveness, and this impairs endometrial receptivity. Therefore, it is feasible that miR-30d dysregulation could affect epithelial-to-mesenchymal transition in the KO murine model, thereby compromising the development of the fetal and maternal vasculature,[54] which facilitates nutrient, gas, and waste exchange. This may explain the smaller size of weaned miR-30d KO mice compared with WT genotype. Further experiments are required to elucidate the function of miR-30d in the process of decidualization in humans to translate this knowledge to the clinical practice.

Strengths and limitations

The use of animal models is of outstanding importance in the areas in which human samples are not accessible for ethical reasons. The strength of this study resides in the use of miR-30d KO mice, which allowed the study of miR-30d deficiency in embryonic implantation and fetal development. Although the use of this murine model provides relevant information to improve the understanding of the embryo—uterine crosstalk, it also presents some difficulties to be extrapolated to humans. The regulation of the molecular machinery responsible for the miR-30d—deficient-implantation phenotype may not be identical in humans. Also, a potential limitation of this study is the use of a whole-body conventional KO, because various phenotypes could coexist, making it difficult to discern the authentic physiological role of the miR-30d in the endometrium.

Conclusion

Our results suggest that in the mouse model, miR-30d plays an important role in regulating embryonic implantation and subsequent fetal development, with special impact of fetal growth restriction. Our results suggest that in the mouse model, miR-30d plays an important role in regulating embryonic implantation and subsequent fetal development, with special impact of fetal growth restriction. These results confirm that the dialogue between the maternal endometrium and the embryo thought miRNAs during the preconception stage plays a role in pregnancy success and fetal growth. ■

Acknowledgments

We thank Fresh Eyes Editing, LLC, for editing this manuscript.

References

1. Barker DJP. The developmental origins of chronic adult disease. Acta Paediatr Suppl 2004;93:26–33.
2. Douglas AJ. Mother-offspring dialogue in early pregnancy: impact of adverse environment on pregnancy maintenance and neurobiology. Prog Neuropsychopharmacol Biol Psychiatry 2011;35:1167–77.
3. Thouas GA, Dominguez F, Green MP, Vilella F, Simón C, Gardner DK. Soluble ligands and their receptors in human embryo development and implantation. Endocr Rev 2014;36:er20141046.
4. Salamonsen LA, Evans J, Nguyen HPT, Edgell TA. The microenvironment of human implantation: determinant of reproductive success. Am J Reprod Immunol 2016;75:218–25.
5. Atwood CS, Vadakkadath Meethal S. The spatiotemporal hormonal orchestration of human folliculogenesis, early embryogenesis and blastocyst implantation. Mol Cell Endocrinol 2016;430:33–48.
6. Bazer FW, Wu G, Spencer TE, Johnson GA, Burghardt RC, Bayless K. Novel pathways for implantation and establishment and maintenance of pregnancy in mammals. Mol Hum Reprod 2010;16:135–52.
7. Robertson SA, Moldenhauer LM. Immunological determinants of implantation success. Int J Dev Biol 2014;58:205–17.
8. Paidas MJ, Krikun G, Huang SJ, et al. A genomic and proteomic investigation of the impact of preimplantation factor on human decidual cells. Am J Obstet Gynecol 2010;202:459.e1–8.
9. Romero R, Grivel J-C, Tarca AL, et al. Evidence of perturbations of the cytokine network in preterm labor. Am J Obstet Gynecol 2015;213:836.e1–18.
10. Galliano D, Pellicer A. MicroRNA and implantation. Fertil Steril 2014;101:1531–44.
11. Mouillet J-F, Ouyang Y, Coyne CB, Sadovsky Y. MicroRNAs in placental health and disease. Am J Obstet Gynecol 2015;213:S163–72.

12. Vilella F, Moreno-Moya JM, Balaguer N, et al. Hsa-miR-30d, secreted by the human endometrium, is taken up by the pre-implantation embryo and might modify its transcriptome. Development 2015;142:3210–21.
13. Simón C, Greening DW, Bolumar D, Balaguer N, Salamonsen LA, Vilella F. Extracellular vesicles in human reproduction in health and disease. Endocr Rev 2018;39:292–332.
14. Bidarimath M, Khalaj K, Wessels JM, Tayade C. MicroRNAs, immune cells and pregnancy. Cell Mol Immunol 2014;11:538–47.
15. Enquobahrie DA, Abetew DF, Sorensen TK, Willoughby D, Chidambaram K, Williams MA. Placental microRNA expression in pregnancies complicated by preeclampsia. Am J Obstet Gynecol 2011;204:178.e12–21.
16. Murphy MS-Q, Casselman RC, Tayade C, Smith GN. Differential expression of plasma microRNA in preeclamptic patients at delivery and 1 year postpartum. Am J Obstet Gynecol 2015;213:367.e1–9.
17. Zemet R, Iskilova M, Brandt B, et al. 624: MicroRNA expression profile in human visceral and subcutaneous adipose tissues during pregnancy: implications for metabolic adaptations to normal gestation and putative novel mechanism of disease in gestational diabetes mellitus. Am J Obstet Gynecol 2018;218:S372–3.
18. Ilekis JV, Tsilou E, Fisher S, et al. Placental origins of adverse pregnancy outcomes: potential molecular targets: an Executive Workshop Summary of the *Eunice Kennedy Shriver* National Institute of Child Health and Human Development. Am J Obstet Gynecol 2016;215:S1–46.
19. Herrero T, Srinivasan S, Treacy R, et al. 512: discovery and verification of maternal serum miRNA biomarkers predictive of preeclampsia. Am J Obstet Gynecol 2019;220:S344.
20. Song P-P, Hu Y, Liu C-M, et al. Embryonic ectoderm development protein is regulated by microRNAs in human neural tube defects. Am J Obstet Gynecol 2011;204:544.e9–17.
21. Altmäe S, Martínez-Conejero JA, Esteban FJ, et al. MicroRNAs miR-30b, miR-30d, and miR-494 regulate human endometrial receptivity. Reprod Sci 2012;20:308–17.
22. Moreno-Moya JM, Ramirez L, Vilella F, et al. Complete method to obtain, culture, and transfer mouse blastocysts nonsurgically to study implantation and development. Fertil Steril 2014;101:e13.
23. Moreno-Moya JM, Vilella F, Martinez S, Pellicer A, Simón C. The transcriptomic and proteomic effects of ectopic overexpression of miR-30d in human endometrial epithelial cells. Mol Hum Reprod 2014;20:550–66.
24. Hayward CE, Lean S, Sibley CP, et al. Placental adaptation: what can we learn from birthweight:placental weight ratio? Front Physiol Front 2016;7:28.
25. Poland BJ. Conception control and embryonic development. Am J Obstet Gynecol 1970;106:365–8.
26. Dey SK, Lim H, Das SK, et al. Molecular cues to implantation. Endocr Rev 2004;25:341–73.
27. Daikoku T, Cha J, Sun X, et al. Conditional deletion of Msx homeobox genes in the uterus inhibits blastocyst implantation by altering uterine receptivity. Dev Cell 2011;21:1014–25.
28. Liu W, Niu Z, Li Q, Pang RTK, Chiu PCN, Yeung WS-B. MicroRNA and Embryo Implantation. Am J Reprod Immunol 2015;75:263–71.
29. Kuokkanen S, Chen B, Ojalvo L, Benard L, Santoro N, Pollard JW. Genomic profiling of microRNAs and messenger RNAs reveals hormonal regulation in microRNA expression in human endometrium. Biol Reprod 2010;82:791–801.
30. Sha A-G, Liu J-L, Jiang X-M, et al. Genome-wide identification of micro-ribonucleic acids associated with human endometrial receptivity in natural and stimulated cycles by deep sequencing. Fertil Steril 2011;96:150–5.
31. Qian K, Hu L, Chen H, et al. Hsa-miR-222 is involved in differentiation of endometrial stromal cells in vitro. Endocrinology 2009;150:4734–43.
32. Wu L, Zhou H, Lin H, et al. Circulating microRNAs are elevated in plasma from severe preeclamptic pregnancies. Reproduction 2012;143:389–97.
33. Mouillet JF, Chu T, Hubel CA, Nelson DM, Parks WT, Sadovsky Y. The levels of hypoxia-regulated microRNAs in plasma of pregnant women with fetal growth restriction. Placenta 2010;31:781–4.
34. Song H, Lim H, Paria BC, et al. Cytosolic phospholipase A2alpha is crucial [correction of A2alpha deficiency is crucial] for "on-time" embryo implantation that directs subsequent development. Development 2002;129:2879–89.
35. Aviram A, Barrett J, Zaltz A, et al. 136: the significance of isolated low placental weight in small-for-gestational age neonates. Am J Obstet Gynecol 2019;220:S104–5.
36. Burton GJ, Jauniaux E. Pathophysiology of placental-derived fetal growth restriction. Am J Obstet Gynecol 2018;218:S745–61.
37. Rosario GX, Stewart CL. The multifaceted actions of leukaemia inhibitory factor in mediating uterine receptivity and embryo implantation. Am J Reprod Immunol 2016;75:246–55.
38. Garrido-Gómez T, Dominguez F, Quiñonero A, et al. Defective decidualization during and after severe preeclampsia reveals a possible maternal contribution to the etiology. Proc Natl Acad Sci USA 2017;1:201706546.
39. Richardson L, Saade GR, Menon R. 1008: progesterone accelerates wound healing in human amniotic epithelial cells through mesenchymal to epithelial transition. Am J Obstet Gynecol 2019;220:S648–9.
40. Chen JR, Cheng JG, Shatzer T, Sewell L, Hernandez L, Stewart CL. Leukemia inhibitory factor can substitute for nidatory estrogen and is essential to inducing a receptive uterus for implantation but is not essential for subsequent embryogenesis. Endocrinology 2000;141:4365–72.
41. Mehta A, Baltimore D. MicroRNAs as regulatory elements in immune system logic. Nat Rev Immunol 2016;16:279–94.
42. Peck BCE, Sincavage J, Feinstein S, et al. miR-30 family controls proliferation and differentiation of intestinal epithelial cell models by directing a broad gene expression program that includes SOX9 and the ubiquitin ligase pathway. J Biol Chem 2016;291:15975–84.
43. Sadowski M, Suryadinata R, Tan AR, Roesley SNA, Sarcevic B. Protein monoubiquitination and polyubiquitination generate structural diversity to control distinct biological processes. IUBMB Life 2012;64:136–42.
44. Wang J, Maldonado MA. The ubiquitin-proteasome system and its role in inflammatory and autoimmune diseases. Cell Mol Immunol 2006;3:255–61.
45. Wegner NT, Mershon JL. Evaluation of leukemia inhibitory factor as a marker of ectopic pregnancy. Am J Obstet Gynecol 2001;184:1074–6.
46. Hambartsoumian E. Endometrial leukemia inhibitory factor (LIF) as a possible cause of unexplained infertility and multiple failures of implantation. Am J Reprod Immunol 1998;39:137–43.
47. Mikolajczyk M, Wirstlein P, Skrzypczak J. The impact of leukemia inhibitory factor in uterine flushing on the reproductive potential of infertile women—a prospective study. Am J Reprod Immunol 2007;58:65–74.
48. Franasiak JM, Holoch KJ, Yuan L, Schammel DP, Young SL, Lessey BA. Prospective assessment of midsecretory endometrial leukemia inhibitor factor expression versus $\alpha v\beta 3$ testing in women with unexplained infertility. Fertil Steril 2014;101:1724–31.
49. Chu B, Zhong L, Dou S, et al. miRNA-181 regulates embryo implantation in mice through targeting leukemia inhibitory factor. J Mol Cell Biol 2015;7:12–22.
50. Dong X, Sui C, Huang K, et al. MicroRNA-223-3p suppresses leukemia inhibitory factor expression and pinopodes formation during embryo implantation in mice. Am J Transl Res 2016;8:1155–63.
51. Cuman C, Van Sinderen M, Gantier MP, et al. Human blastocyst secreted microRNA regulate endometrial epithelial cell adhesion. EBioMedicine 2015;2:1528–35.
52. Burns GW, Brooks KE, Spencer TE. Extracellular vesicles originate from the conceptus and uterus during early pregnancy in sheep. Biol Reprod 2016;94:56.
53. Cai J-L, Liu L-L, Hu Y, et al. Polychlorinated biphenyls impair endometrial receptivity in vitro via regulating mir-30d expression and epithelial mesenchymal transition. Toxicology 2016;365:25–34.
54. Niu Z-R, Han T, Sun X-L, Luan L-X, Gou W-L, Zhu X-M. MicroRNA-30a-3p is overexpressed in the placentas of patients with preeclampsia and affects trophoblast invasion and apoptosis by its effects on IGF-1. Am J Obstet Gynecol 2018;218:249.e1–12.

Author and article information

From the Department of Pediatrics, Obstetrics, and Gynecology, Universidad de Valencia, Valencia, Spain (Dr

Balaguer); R&D Department, Igenomix Foundation, Valencia, Spain (Drs Moreno and Vilella, Ms Herrero and Gonzáléz-Monfort); Instituto de Investigación Sanitaria Hospital Clínico (INCLIVA), Valencia, Spain (Dr Vilella); Igenomix S.L., Valencia, Spain (Dr Simon); Department of Pediatrics, Obstetrics and Gynecology, Universidad de Valencia, INCLIVA, Valencia, Spain (Dr Simon); and Department of Obstetrics and Gynecology, School of Medicine, Stanford University, Stanford, CA (Dr Simon).

[1]These authors contributed equally to this article.

Received Aug. 29, 2018; revised Jan. 30, 2019; accepted Feb. 22, 2019.

I.M., M.H., M.G., and C.S. are employed by Igenomix S.L. N.B. and F.V. report no conflict of interest.

This work was supported by the Miguel Servet Program Type II of Instituto de Salud Carlos III (CPII18/00020); FIS project (PI18/00957) to F.V.; the 'Atracció de Talent' Program from VLC-CAMPUS (UV-INV-PREDOC14-178329) to N.B.; and MINECO/FEDER Grant [SAF2015-67154-R] to C.S.

Preliminary results were presented at the 64th Annual Scientific Meeting of the Society for Reproduction Investigation, Orlando, FL, March 15-18, 2015, and at the 2018 Gordon Research Conference on Mammalian Reproduction, Barga, Italy, July 29-Aug. 3, 2018.

Corresponding author: Felipe Vilella, PhD. felipe.vilella@igenomix.com

Glossary

miR-30d: MicroRNA miR-30d belongs to the microRNA 30 family. This family includes 5 members (miR-30a—miR-30e) derived from 3 miRNA clusters. The expression of its members has been described to be greater during the receptivity period in both mice and humans. Thus, the endometrial epithelial cells of the receptive uteri present greater levels of miR-30b and miR-30d. Consistently, the expression of these miRNAs is downregulated in decidualized endometrial stromal cells relative to their nondecidualized counterparts. In primary human endometrial epithelial cells, transient overexpression of miR-30d activates genes and proteins involved in proliferation, hormonal responses, and methylation status. In particular, the presence of miR-30d during the WOI favors the expression of adhesion molecules, thus leading to an increase of the implantation rates of murine embryos and embryos surrogates derived from a human trophoblastic cell line.

IUGR: Intrauterine growth restriction (IUGR) refers to a condition in which a fetus is unable to achieve its genetically determined potential size. This functional definition aims to identify a population of fetuses at risk for modifiable poor outcomes. This definition excludes those fetuses that are small for gestational age (SGA) but are not pathologically small. SGA is defined as growth at the 10th or less percentile for weight of all fetuses at that gestational age. Importantly, not all fetuses that are SGA are pathologically growth restricted. Similarly, not all fetuses that have not achieved their genetic growth potential are in less than the 10th percentile for estimated fetal weight (EFW).

***Cox2* (*Ptgs2*):** Cyclooxygenase 2 is one of the most common COX-derived prostaglandins and is spatiotemporally expressed during pregnancy. *Cox2* is induced in the luminal epithelium and underlying stroma at embryonic attachment sites, signifying that it likely has roles in attachment and localized endometrial vascular permeability. *Cox2* deficiency has been associated with implantation failure. Upon attachment, *Cox2* localizes to antimesometrial decidua, but by day 6 of pregnancy, it displaces to the opposite (mesometrial) side. $Ptgs2^{-/-}$ females also show defective ovulation, fertilization, decidualization, and placentation, thus highlighting the roles of Cox2-derived prostaglandin signaling at several stages of pregnancy. In addition, epithelial sodium channels must be activated to induce Cox2 at the implantation stage.

***Lif*:** Leukemia inhibitory factor is a proinflammatory factor that regulates proliferation, differentiation, and cell survival and whose expression appears to be maternally controlled and becomes considerably increased during the WOI. LIF acts by binding to its receptor, LIFR, and co-receptor, gp130; this binding triggers several signaling pathways, including the JAK/STAT, mitogen-activated protein kinase, and phosphatidylinositol-3 kinase pathways. The phenotype of Lif knockout mice demonstrates the importance of LIF in reproduction: females are fertile, but their blastocysts fail to implant. These discoveries prompted the implementation of clinical trials investigating the effect of recombinant human LIF administration during the luteal phase of women with implantation failure; however, no noticeable improvements in pregnancy rates were achieved.

Msx1 and Msx2: Muscle segment homeobox gene family members *Msx1* and *Msx2* are known tissue morphogenesis regulators and play critical roles in uterine stromal-epithelial interactions. During pregnancy, *Msx1* and *Msx2* expression is confined to the luminal epithelium and glandular epithelium on day 3 and 4, but are markedly downregulated on the evening of day 4, coinciding with blastocyst attachment. Conditional deletion of either *Msx1* or *Msx2* results in subfertility, whereas double knockout of both *Msx1* and *Msx2* causes infertility, suggesting that a compensatory mechanism exists between MSX1 and MSX2.

ESR: Estrogen receptor. ESRα and ESRβ are transcription factors which in the absence of estrogen are mainly present in the cytoplasm. Hormone binding favors receptor activation, resulting in its dimerization and subsequent translocation into the nucleus. Once activated, they can bind to specific genomic sites to enable or repress the expression of their target genes. ESRα is considered the predominant ESR isoform because its loss results in female infertility and insensitivity to the mitogenic effects of E_2. In contrast ESRβ ablation does not seem to affect uterine functionality but does negatively impact fertility by causing an ovarian defect. Surprisingly, loss of epithelial ESRα does not prevent estrogen-induced epithelial cell proliferation, suggesting that the action of ESRα upon the stroma is critical for mediating this event.

PGR: Progesterone receptor. Progesterone receptor isoform A and progesterone receptor isoform B are the main isoforms of the PGR. As in the case of the ESR, hormone binding favors receptor activation, resulting in its dimerization and subsequent translocation into the nucleus. Once activated, they can bind to specific genomic sites to enable or repress the expression of their target genes. The expression of epithelial PGR appears to increase in the days preceding implantation, suggesting its relevance in establishing uterine receptivity. Specifically, PGR expression decreases in the uterine epithelium at the time of attachment but simultaneously increases in the endometrial stroma surrounding the implantation site. One of the leading functions driven by endometrial PGR is the induction of Indian Hedgehog) in the epithelium during the pre-receptive phase. Mouse models lacking functional PGR (PRKO) are characterized by their infertility, which is caused by an ovulation defect. Specially, their uteri are hyperplastic and nonreceptive to implanting embryos. Interestingly, these mutant mice also fail to trigger a decidual response following artificial stimulation of their hormone-primed uteri. In addition, mice lacking PR exclusively in the epithelium show clear signs of infertility associated with the existence of persistent proliferation of the luminal epithelium.

EMT: Epithelial to mesenchymal transition (EMT) is the process by which an immotile, polarized, epithelial cell undergoes several biochemical changes to acquire mesenchymal cell characteristics, which include the ability to migrate and invade. During normal placental development, villous cytotrophoblast differentiates into more invasive extravillous trophoblast, a process marked by an EMT. Nevertheless, while EMT is tightly regulated and precisely orchestrated during normal development, the dysregulation of EMT is associated with the pathologic processes of tumor metastasis and cancer progression, as well as with pregnancy disorders such as preeclampsia, fetal growth restriction and endometriosis.

Actin: Beta-Actin (42 kDa) is commonly chosen as a loading control in western blotting due to its general expression across all eukaryotic cell types. The expression levels of this protein do not vary drastically due to cellular treatment, which is another reason the protein makes a suitable control.

Calnexin: Calnexin is a chaperone characterized by its interaction with newly synthesized glycoproteins in the endoplasmic reticulum. It may act in assisting protein assembly and/or in the retention within the ER of unassembled protein subunits. In western blotting is usually used as a representative marker of proteins belonging to the membranous organelles fraction.

ZO-1: Zonula Occludens-1 is a known key regulator of tight junction formation. In the mouse uterus during the peri-implantation period, preimplantation uterine epithelial cells express both ZO-1 and E-cadherin. As implantation progresses, ZO-1 and E-cadherin are expressed in stromal cells of the primary decidual zone. Therefore, as trophoblast invasion takes place, these two molecules are expressed in stroma in advance of the invading trophoblast cells.

MirC26tm1Mtm/Mmjax: A microRNA cluster 26 (miR-30b/miR-30d) conditional mutant mice designed to generate a null allele or a *lacZ* tagged null allele when combined with Flp or Cre recombinase expressing strains. *LacZ* expression is widespread. This mutant mouse strain is useful in studies of microRNA biology

Pseudopregnancy: Pseudopregnancy is a term used to describe a false pregnancy in several mammalian species. It is a physical state whereby all the signs and symptoms of pregnancy are exhibited, except for the presence of a fetus. Pseudopregnant mouse defines a female mouse after copulation with a vasectomized male. The mouse behaves hormonally pregnant allowing its use as a recipient for embryos; e.g. for chimera production.

Decidualization: Decidualization is the differentiation of elongated, fibroblast-like mesenchymal cells in the uterine stroma to rounded, epithelioid-like cells during the menstrual cycle and pregnancy. This morphological change initiates during the mid-secretory phase as a result of elevated progesterone levels and begins with stromal cells surrounding the spiral arteries in the upper two-thirds of the endometrium, regardless of the presence or absence of a conceptus.

SUPPLEMENTAL FIGURE 1
Analysis of receptivity markers in pregnant female

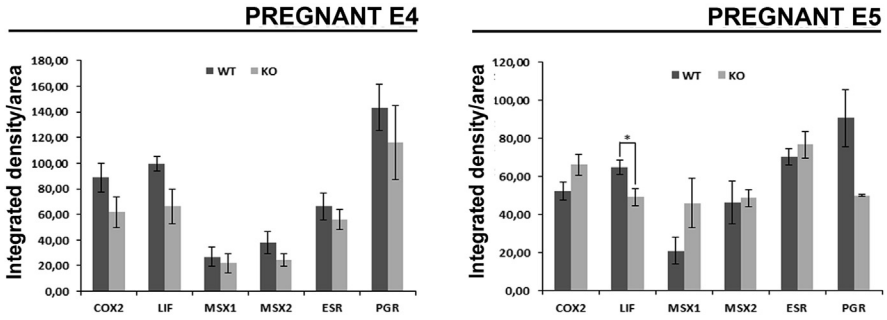

Right graph integrates fluorescence value density/area calculated for every receptivity marker at day 4 of pregnancy. In general, all the mean fluorescence intensity values decreased for all the receptivity markers, but this decrease was not significant. *Left graph* integrates density/area calculated for every receptivity marker at day 5 of pregnancy. The fluorescence intensity value of LIF was significantly downregulated in KO uteri (64.73 $\pm$ 3.86 vs 49.15 $\pm$ 9.05; $P = .034$). For the rest of the markers, differences were not significant

KO, knockout; *LIF*, leukemia inhibitory factor.

Balaguer et al. MicroRNA-30d deficiency during preconception affects endometrial receptivity by decreasing implantation rates and impairing fetal growth. Am J Obstet Gynecol 2019.

SUPPLEMENTARY TABLE 1
Primers for RT-qPCR

Gene name	Forward	Reverse
Cox2	AACCGAGTCGTTCTGCCAAT	CTAGGGAGGGGACTGCTCAT
Lif	TGTCGCCTAGATTTACCC	CACAATCCCTGCATCTCATC
Msx1	TCTCGGCCATTTCTCAGTTCG	CCGATCTAGTTTCTCGGGGC
Msx2	TCGTCAAGCCCTTCGAGACC	TGGTGGGGCTCATATGTCTGGG
Esr	TGCCAAGGAGACTCGCTACT	CTCCGGTTCTTGTCAATGGT
Pgr	CACAAAGCCTGACACTTCCA	AAACACCATCAGGCTCATCC
Act	GATCATTGCTCCTCCTGAGC	AGTCCGCCTAGAAGCACTTG

RT-qPCR, real-time quantitative polymerase chain reaction.

Balaguer et al. MicroRNA-30d deficiency during preconception affects endometrial receptivity by decreasing implantation rates and impairing fetal growth. Am J Obstet Gynecol 2019.